Exo-Glove PM: An Easily Customizable Modularized Pneumatic Assistive Glove

Sung-Sik Yun, Brian Byunghyun Kang, and Kyu-Jin Cho, *Member, IEEE*

***Abstract*—Customization is an important issue for assistive gloves because it affects glove performance. In this letter, we propose an assembly based customizable soft pneumatic assistive glove, named Exo-Glove PM. Pneumatic soft robots generally consist of a single structure with embedded actuators. However, when assembled, the region where the assemblies are connected easily undergoes large stress concentration that leads to failure. To overcome this issue, we have developed a hybrid actuator module that combines a soft actuation structure and rigid joining methods. In general, rigid joining methods require a bulky design to enable easy assembly, but Exo-Glove PM is designed to create pathways for assembly tools to access the bolt heads by bending certain parts. This novel way of joining assemblies allows soft robots to be built of multiple parts while minimizing the volume. It ensures small module size and enables modules to cover a wide range of hand sizes; the distance between each module is matched to the length of the user's phalanges using spacers. This approach allows users to customize the glove by assembly of standardized modules and maximizes the comfort and the performance of the glove without custom manufacturing and, thus, reduces costs.**

***Index Terms*—Physically assistive devices, prosthetics and exoskeletons, rehabilitation robotics.**

I. Introduction

TO BUILD an effective and comfortable wearable robots, the size of the robot must be matched to the wearer. However, fitting a robotic glove to a hand is a particularly difficult problem, for the following reasons. First, hand size and shape vary a great deal. Consider, for example, the size difference between men and women and the different finger lengths and finger-palm ratios among people. Second, hand size changes as people age. Finally, hand shape and joint stiffness among patients with the same injury varies, depending on the duration and degree of patient's rehabilitation exercise. Although today's commercialized robotic assistive gloves are produced in standard sizes, customization is required to provide the best-possible functioning for each patient [1], [2].

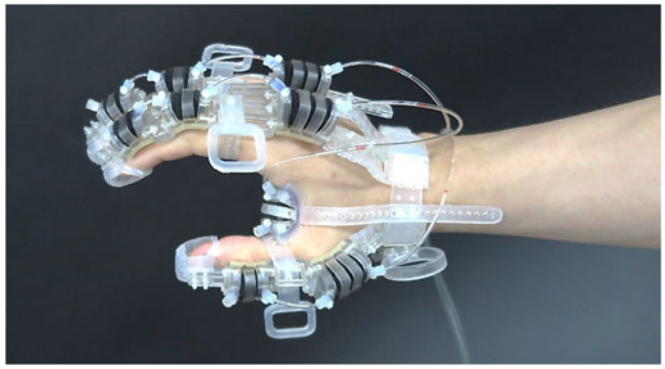

Fig. 1. Prototype of Exo-Glove PM.

There are several types of robotic assistive gloves: the rigid linkage type, the soft tendon–driven type, and the soft pneumatic type. Each has its own size-matching solution.

Some rigid linkage gloves can be matched to users by changing the length and angle of their links [3], [4]. Other rigid linkage gloves, such as HEXOTRAC [5] and UT Hand Exoskeleton [6] has sufficiently large frame and change their control trajectory to accommodate any hand size.

In the case of soft tendon–driven gloves, Exo-Glove Poly uses a stretchable design and elastic material to allow it to fit various hand sizes. Glove size can be matched to hand size by stretching the finger straps [7].

Some soft pneumatic gloves imitate the wearer's hand movement by employing a strain-limiting fabric at the bending actuators where the wearer's finger joints are positioned [8], [9]. Some gloves can be customized by changing mold design parameters to fit the user's hand size [10]–[12].

Although these methods are good solutions for customization, they have some issues. For example, link design changes can cause unintended behavior changes in rigid linkage gloves. Gloves that are very large (e.g., HEXOTRAC and UT Hand Exoskeleton) are bulky and heavy, which reduces wearability. The stretchable structure of soft tendon–driven gloves can also cause unintended behavior changes because stretching can change the tendon path. Customizing soft pneumatic gloves requires that parts be specially manufactured to fit users and necessitates communication between users and the manufacturer, all of which hinders automated fabrication and increases cost and required lead time for customers.

In this letter we present a new soft pneumatic modular assistive glove, Exo-Glove PM, which relies on a novel customization

Manuscript received September 10, 2016; accepted February 7, 2017. Date of publication March 6, 2017; date of current version May 16, 2017. This letter was recommended for publication by Associate Editor K. Ogata and Editor K. Masamune upon evaluation of the reviewers' comments. This work was supported in part by the Technology Innovation Program (10051287, Development of fundamental technology of soft robotics for advanced soft gripper) funded by the Ministry of Trade, Industry, and Energy (MI, South Korea) and in part by the National Research Foundation of Korea (NRF) funded by the Korean Government (MSIP) under Grant NRF-2016R1A5A1938472.

The authors are with the Biorobotics Laboratory, School of Mechanical and Aerospace Engineering/IAMD, Seoul National University, Seoul 151-742, South Korea (e-mail: yss1215@snu.ac.kr; brianbkang@snu.ac.kr; kjcho@snu.ac.kr).

This paper has supplemental downloadable multimedia material available at http://ieeexplore.ieee.org, provided by the authors. The Supplementary Material contains a video demonstrating the assembly process and grip performance of Exo-Glove PM. This material is 29.7 MB in size.

Digital Object Identifier 10.1109/LRA.2017.2678545

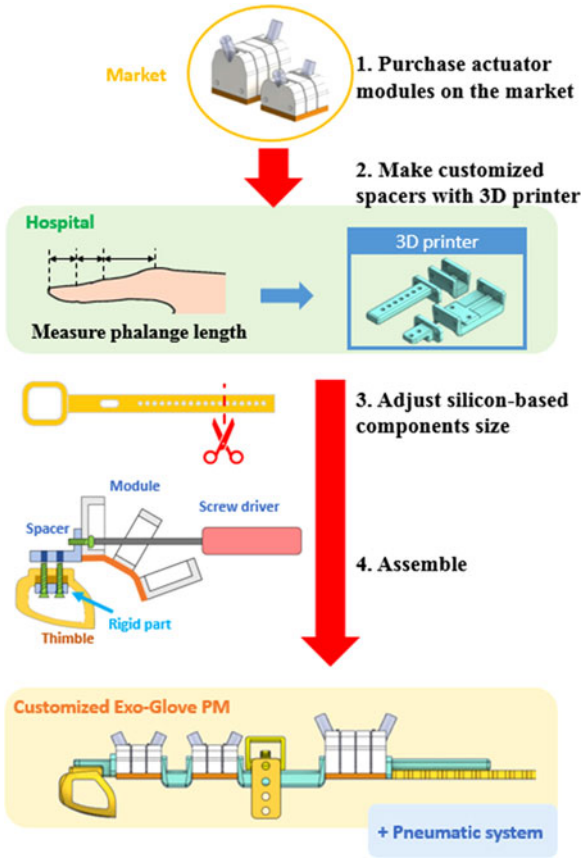

Fig. 2. Customization process.

method that eliminates the need for custom manufacturing and thus reduces costs (see Fig. 1). By matching the intervals of standardized actuator modules to the length of the user's phalanges, this glove can be customized to fit various patients. Glove size is adjusted using spacers. In addition, a novel way of joining assemblies while deforming the structure allows the glove to be built of multiple parts while minimizing the volume. Since this glove is built with standardized actuator modules, repair costs are also significantly reduced. Instead of replacing the whole actuator package, a glove can be repaired by replacing only the affected actuator modules. Because the replacement process is simple, users or their assistants can fix their gloves themselves at home and continue to use them.

In this letter, we describe the components of Exo-Glove PM and explain how it can be customized. To predict actuator module performance and provide users with information about actuator module selection, we analyzed the module by mechanical modeling and verified its performance experimentally via hand movement observations, measuring maximum endurable weight, and a grasping test. The letter concludes with a discussion of our results and implications for future work.

II. Assembly-Based Customization

Exo-Glove PM is an assembly-based customizable soft pneumatic assistive glove. The concept behind this assistive glove is maximizing performance by customizing standardized actuator modules to match the needs of the user through assembly.

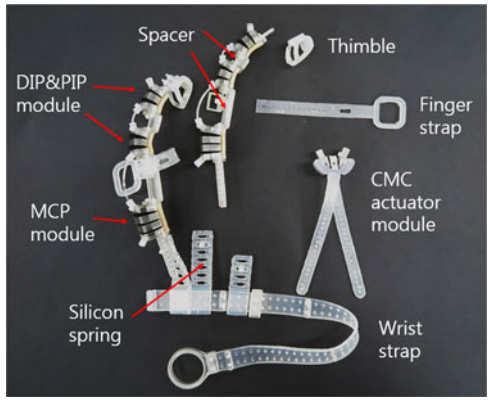

Fig. 3. Components of Exo-Glove PM.

Fig. 2 shows the process of customizing Exo-Glove PM. The glove is composed of actuator modules, spacers, and silicone-based components (see Fig. 3).

The first step in customizing the glove is to choose the actuator module according to preferred strength or size. A range of standardized actuator modules are available.

Spacer length must be customized for each patient. Patients can make their own spacers with a three-dimensional (3D) printer at a hospital, a health center, or any other location where they have access to a printer.

After actuator modules and spacers are assembled, the silicone-based components are cut to the proper size with scissors. The supplied components are long enough to be cut to fit a range of finger sizes. Then the spacers must be attached to the actuators using bolts and nuts. This completes the customization process.

Lastly, after connecting the pneumatic system hoses to the glove and tightening hose entrances with cable ties, patients can use their customized assistive glove.

III. Exo-Glove PM Components

A. Actuator Module

Pneumatic soft robots generally consist of a single structure with embedded actuators. However, when assembled, the region where the assemblies are connected easily undergoes large stress concentration which leads to failure. To overcome this issue, we have developed a hybrid actuator module that combines a soft actuation structure and rigid joining methods.

The actuator module is composed of an outer shell whose rigid tunnel-shaped parts are attached to a rubber sheet and a polymer tube covered with fabric. Because the rubber sheet restricts extension of the actuator bottom, the actuator bends when air is injected. Because the modules push each other through a rigid surface, the actuator can display good force transmission performance while maintaining high degrees of freedom (DOF) when passively bent or twisted.

Actuator module performance can be altered by changing the outer shell design, using an identical polymer tube and fabric. A bent actuator module should be able to fit various finger joint curvatures. We used three 5 mm-long tunnel-shaped parts as actuators for the distal interphalangeal (DIP), proximal interphalangeal (PIP), and interphalangeal (IP) joints [see Fig. 4(d)]. The actuator used for the metacarpophalangeal (MCP) joints consists of four of these tunnel-shaped parts. The curvature of a

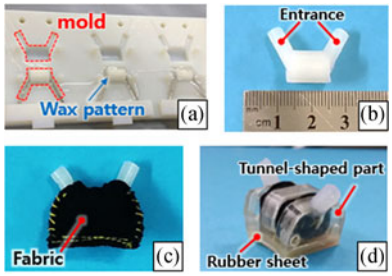

Fig. 4. Actuator module fabrication process. (a) Polymer tube molding process. (b) Polymer tube. (c) Tube covered with fabric. (d) Combination of tube and outer shell (DIP and PIP module).

module is determined by the number of its tunnel-shaped parts. Theoretically, the radius of curvature of each actuator module is 6.7 mm and 10.3 mm at 90°. However, thanks to the soft properties of the module, the actuators are adaptable for various finger joint curvatures and work well for people with different hand sizes.

Because the initial module size is small, the deformation rate of a tube exceeds 300% when it is bent up to 90°. To bear such a large deformation, we made the polymer tubes with Dragon Skin 10 (Smooth-On, Inc.), which can be elongated up to 1000%.

However, the hardness of Dragon Skin 10 is low, so it is vulnerable to high air pressure. To solve this problem, we wrapped the polymer tubes with fabric. The fabric we used exhibits anisotropy: It extends easily in the lengthwise direction and poorly in the radial direction. Therefore, the fabric can prevent over-expansion of the tube and concentrate force into the lengthwise direction. We also made the cylindrical entrances of the tubes with Dragon Skin 30 to prevent bursting.

We used a wax pattern and 3D-printed molds [see Fig. 4(a)] to make the polymer tube [see Fig. 4(b)]. Cylindrical solid wax was used as a mold pattern because the tube is too small to be completed with a general molding process. After covering the tube with fabric [see Fig. 4(c)], it is inserted into an outer shell [see Fig. 4(d)]. Thanks to its unique Y-shaped design, the tube can be structurally fixed to the outer shell. An air hose can be connected to the tube by pushing it into an entrance.

Modules are connected to each other directly or through a spacer by rigid connecting elements. In general, the design of products that use rigid joining methods is constrained by the need to ensure that they can be easily assembled. This results in a bulkier design compared to products produced as one part. Since Exo-Glove PM is designed to be able to create pathways for assembly tools to access the bolt heads by bending rubber sheet, we have been able to develop an assembly that minimizes volume (see the assembly process illustrated in Fig. 2).

Actuator modules are divided into four finger actuators (DIP, PIP, MCP, IP) and a carpometacarpal (CMC) joint actuator. The basic composition and the operating principle of these actuators are identical. The only difference between them is that the outer shell of the CMC actuator is saddle shaped. This actuator is positioned between the thumb and the index finger; this is the most effective position for transmitting force to open the CMC joint.

B. Spacer

Spacers hold the distance between two actuator modules at certain required values. By regulating module intervals with a spacer, the glove can be customized to individual users. Spacers of different sizes can be made with a 3D printer. They can also be manufactured and sold as a standardized industrial product.

Spacers are needed for the intermediate phalange and the proximal phalange. To determine the correct spacer length, the length of each subject's phalange is measured with the hand fully extended (the length of the intermediate and proximal phalange will be expressed as L_i and L_p). In the human hand, the length of the finger increases when the fingers bend. To obtain a large ROM of the finger, the actuator package must be longer than the extended finger length because the spacer cannot extend. Experiments on users' satisfaction when using the glove led to the development of two formulas for determining the appropriate spacer length to use when customizing a glove:

$$\mathrm{S}_i = \mathrm{L}_i - 11 \text{ mm} \tag{1}$$

$$\mathrm{S}_p = \mathrm{L}_p - 12.5 \text{ mm} \tag{2}$$

where S_i is the length of the intermediate phalange spacer and S_p is the length of the proximal phalange spacer.

We evaluated the validity of these formulas by asking three healthy subjects with differing hand sizes to perform a grasping test (see Section V-C). At present we are measuring phalange length with measuring tape.

The main issue in using spacers was that they must be able to regulate module distance continuously from zero to infinity in order to cover the wide range of hand sizes.

There are existing studies describing soft pneumatic module connections. However, neither magnets [13] nor electroadhesive pads [14] are robust enough to transmit large forces. SoBL (Soft Robotic Blocks) use three connecting mechanisms: a screw thread, a push fitting, and a bistable junction [15]. The screw thread and push fitting mechanisms are similar to those used in Exo-Glove PM in that they adopt an existing rigid element. However, it is difficult to adjust the distance between SoBL as desired. The body of the bistable junctions is entirely made of elastomer, which leads to a bulky connector.

We were able to connect the modules using off-the-shelf bolts and nuts. The distance between the modules can be adjusted as desired by using different connection methods, as show in Fig. 5.

C. Silicone-Based Glove Components

The glove's thimble, finger strap, and wrist strap are made of silicone (KE-1300T, Shinetsu). These components fix the glove to the patient's hand and are designed to be easy to don and doff. These elements fix the actuator firmly to the hand so that the torque of the actuator can be transmitted to the finger. A silicone spring that extends when the fingers bend helps to extend the fingers by applying elastic force. Fig. 3 depicts these silicone-based components, which were inspired by preceding research [7]. Thanks to the properties of silicone, glove performance is improved by high friction. Also, the silicone components do not absorb sweat and are washable, helping to keep the glove hygienic.

D. Pneumatic System

The glove comes with a portable pneumatic system composed of three serially connected miniature air pumps (DAP-370P, Motorbank), an 11.1 V 800 mAh lithium-polymer battery, a control

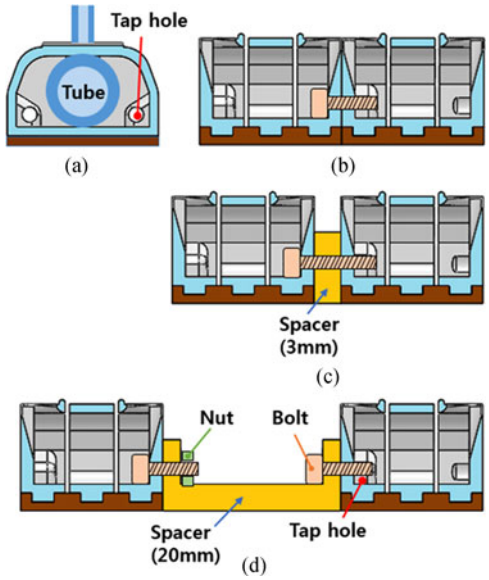

Fig. 5. Module distance regulation. (a) Module cross section. (b) 0 mm interval. (c) 3 mm interval. (d) 20 mm interval.

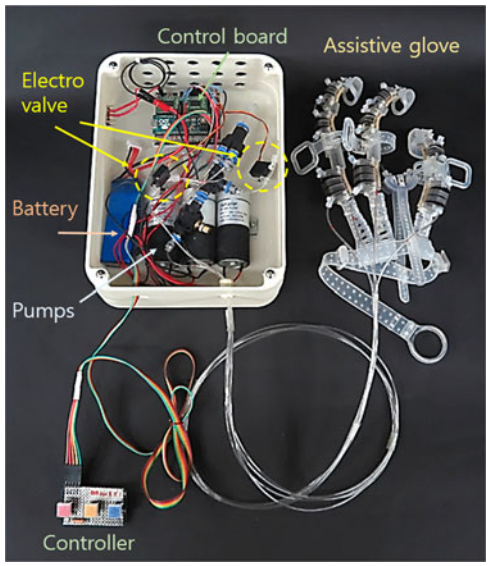

Fig. 6. Portable pneumatic system.

board (Arduino MICRO, Arduino), and two tiny servo motors (PZ-15320A1, DRCmall). To minimize the system's weight, we made a light (3.2 g) electro valve from a tiny servo motor and a 2 mm-diameter air hose, instead of using a solenoid valve. The servo motor unfolds or folds the hose to allow or block air flow through the hose. The electro valve can block over 400 kPa (4bar) pressure. Each pump can supply 100 kPa (1bar) air, and the series of three pumps can supply pressurized air up to 300 kPa (3bar). The total weight of the system is 600 g (350 g without its case). The system does not need to store pressurized air because the glove consumes little air, only at its joints. The system includes a controller with three switches, each controlling a different function: general grasp (power grasp and pinch grasp), lateral pinch, and extension. Pushing a switch causes pressure to gradually grow, which allows users to control grasping force by varying the length of time that they push a switch. The complete portable pneumatic system is shown in Fig. 6.

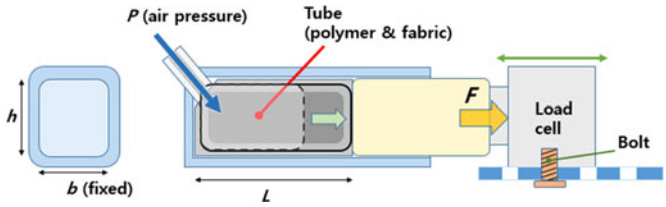

Fig. 7. Tube performance experiment setup.

TABLE I
COEFFICIENTS OF EQUATION (3)

Height (*h*)	*A*	*B*	*C*	*D*
8 mm	−0.5952	14.9860	0.1389	−4.5196
9 mm	−0.5636	15.1717	0.0446	−3.1009
10 mm	−0.5488	15.6620	0.0650	−3.7476
11 mm	−0.6692	19.1896	0.1062	−4.9786

IV. ACTUATOR MODELING AND ANALYSIS

One advantage of this modularized assistive glove is that users can choose module sizes according to their preferred strength. Because the modules are activated by air pressure, a large module provides more bending torque than a smaller one, in accordance with Pascal's law. To select the proper module size, it is necessary to predict the bending torques of different size modules. Therefore, we created a mechanical model of the actuator modules that tested two bending conditions: a 0° joint angle and a large joint angle ($\theta >= 30°$).

Before working on the model, we performed a simple experiment to determine the characteristics of the fabric-covered polymer tube (see Fig. 7). We put a tube into a tetragonal cylinder and used a load cell (333FB Cell, Ktoyo Co., Ltd., Korea) to measure its length-directional force (F) for a certain locked cylinder length (L) condition cell. We conducted the experiment at 1-3bar (300 kPa) pressure (P) with a 0.5bar (50 kPa) interval, a 15-24 mm cylinder length (L) with a 3 mm interval, and a 8-11 mm cylinder height (h) with a 1 mm interval. The width (b) was fixed at 15 mm. The experimental data was linearly distributed, so F can be approximated as follows:

$$F = A \cdot P \cdot L + B \cdot P + C \cdot L + D \tag{3}$$

where A, B, C, and D are determined by h (listed in Table I). Units of measure in the equation are as follows: P is bar, L is mm, h is mm, and F is N.

Experimental F values and the approximated F function are expressed in plots in Fig. 8. The plots are almost coincident. Because radial expansion of the tube is restricted by fabric, this function can be used for actuator modeling. The F function shows the spring characteristics of a pressurized polymer tube. We can assume that the initial length and spring coefficient increase along with inner pressure. Therefore, we can regard the force of the expanded tube as a deformed spring force and simplify the equations. In fact, the meaning of coefficients A, B, C, and D is vague because the coefficients can be changed along the units of P and L in (3).

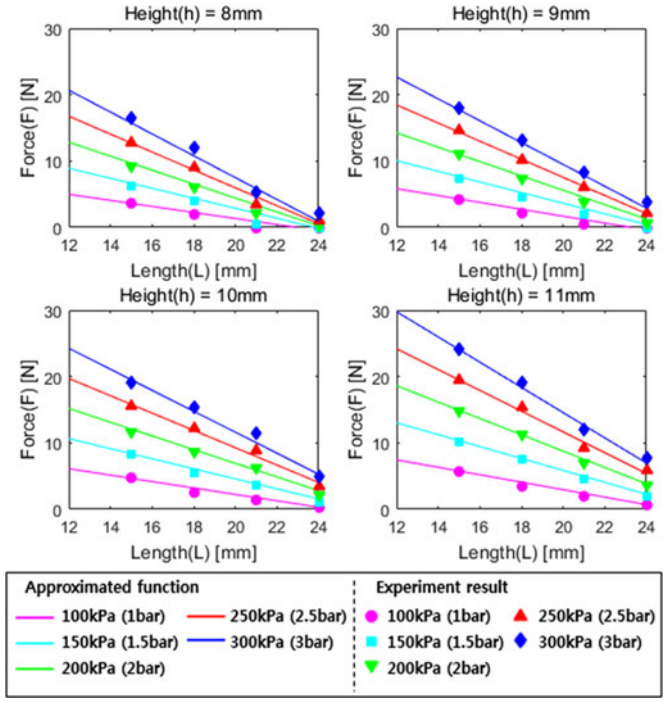

Fig. 8. Evaluation of the suitability of the length-directional force approximated function.

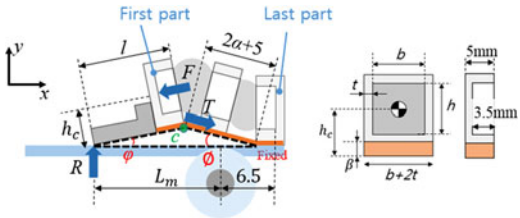

Fig. 9. FBD of the actuator module at 0° joint angle.

A. Bending Torque Over Air Pressure at a Fixed 0° Joint Angle

When the joint angle is 0°, the actuator module is tilted in angle φ when it presses the finger. Fig. 9 shows a free body diagram (FBD) of this situation. The force and moment equilibrium equations for pressing the load cell are as follows:

$$\sum F_x = 0 : \quad T\cos\phi = F\cos\varphi \tag{4}$$

$$\sum F_y = 0 : \quad R = F\sin\varphi + T\sin\phi \tag{5}$$

$$\sum M_c = 0 : \quad Rl\cos\varphi = Fh_c \tag{6}$$

where R is the reaction force of the finger, T is the elastic force of the rubber sheet, and ϕ is the angle of the rubber sheet.

Also, based on the module's shape in the equilibrium condition, an additional equation can be found using the law of sines:

$$\frac{\sin\varphi}{2\alpha+5} = \frac{\sin\phi}{l} \tag{7}$$

$$\mathrm{L} = 2\alpha{+}12 \tag{8}$$

The rubber sheet to which the outer shell of the actuators is attached is composed of VytaFlex 30 (Smooth-On, Inc.), which has a 100% modulus of 65 psi (0.45 N/mm^2). We set the 100% modulus of VytaFlex 30 as a Young's modulus (E). The elastic force of the rubber sheet can be expressed as follows:

$$T = EA\varepsilon = E\cdot(b+2t)\cdot\beta\cdot\frac{\alpha-\alpha_0}{\alpha_0} \tag{9}$$

where $E = 0.45$ N/mm^2, $b = 15$ mm, $t = 1$ mm, $\beta = 2$ mm, and $\alpha_0 = 0.8$ mm. α is the distance between the two tunnel parts.

Additionally, we can find the longitudinal force of the tube by substituting (8) for F in Equation (3). Finally, the bending torque (τ) of the actuator module can be obtained by the following equations:

$$\tau = L_m \cdot R \tag{10}$$

$$L_m = l\cos\varphi{+}(2\alpha+5)\cos\phi\text{ - }3 \tag{11}$$

By combining Equations (3)–(11), the bending torque can be obtained. Because the simultaneous equation is complex to solve, we obtained the values via a numerical method.

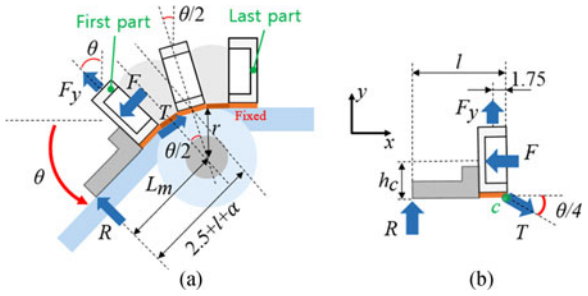

Fig. 10. Schematic diagram of an actuator module bending at a large angle (θ). (a) FBD of an actuator module at a large angle (θ). (b) FBD of the first tunnel-shaped part of the actuator in (a).

B. Bending Torque Over a Large Joint Angle

The process of actuator modeling for a large joint angle ($\theta >= 30°$) is similar to that for the 0° case but has some differences. First, actuator performance is influenced by joint radius. Second, the amount of tilting by the actuator is so small that it can be ignored. Lastly, the expanded tube applies not only longitudinal force but also tangential force. We developed an FBD (see Fig. 10) and then used force and moment equilibrium equations as the terms of the first tunnel-shaped part of the module as follows:

$$\sum F_x = 0 : \quad F = T\cos\frac{\theta}{4} \tag{12}$$

$$\sum F_y = 0 : \quad R + F_y = T\sin\frac{\theta}{4} \tag{13}$$

$$\sum M_c = 0 : \quad Rl + 1.75F_y = h_cF \tag{14}$$

Note that (3) and (9) can be used without change in this calculation. It is necessary to consider tube length (L) because the module is bent. We used an average of the under (d_1) and the upper (d_2) fabric lengths for one gap to determine the entire tube length (L) [see Fig. 11(a)]. However, finding d_2 is complicated because the fabric is not flat at the upper side of the module, so we simplified the expanded fabric shape as a trapezium by adopting a fabric expansion factor (f_e) [see Fig. 11(b)]. We

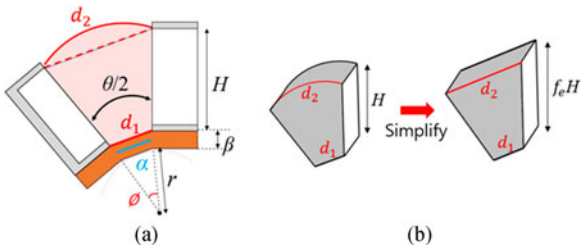

Fig. 11. Schematic diagram of expanded fabric. (a) Expanded fabric in a single gap. (b) Simplified fabric shape (trapezium).

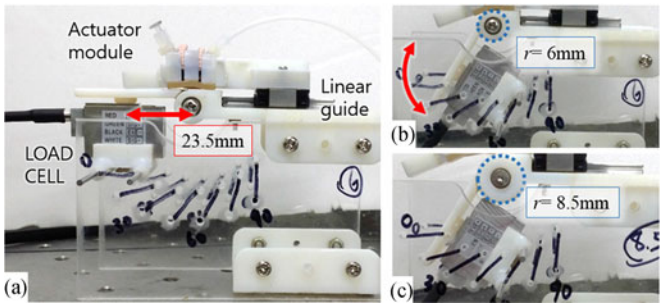

Fig. 12. Experimental setups for measuring actuator module bending torque. (a) Setup components. (b) Setup with a 6 mm joint radius. (c) Setup with an 8.5 mm joint radius.

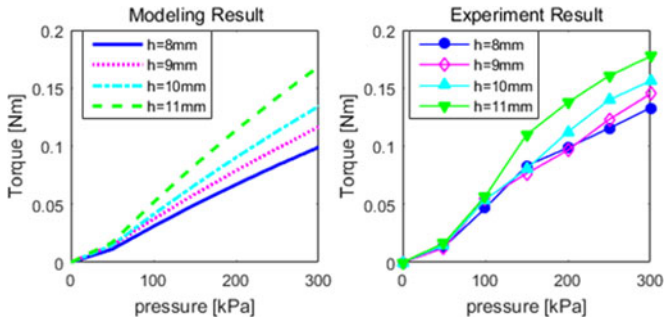

Fig. 13. Comparison of modeling and experimental results for actuator bending torque over pressure, at 0°.

found that 1.25 is the proper value for f_e in our module. This value is determined by the directional property of the fabric. Fabric length can be expressed through the following equations:

$$\left(r + \frac{1}{2}\beta\right) : \alpha = (r+\beta) : d_1 \tag{15}$$

$$\therefore\ d_1 = \frac{(r+\beta)}{(r+\frac{1}{2}\beta)} \cdot \alpha \tag{16}$$

$$d_2 = d_1 + 2f_eH\sin\frac{\theta}{4},\ H = h + t \tag{17}$$

$$L = 12 + 2 \cdot \frac{(d_1+d_2)}{2} \tag{18}$$

Finally, the bending torque (τ) of the actuator module can be obtained by the following equations:

$$\tau = L_m \cdot R \tag{19}$$

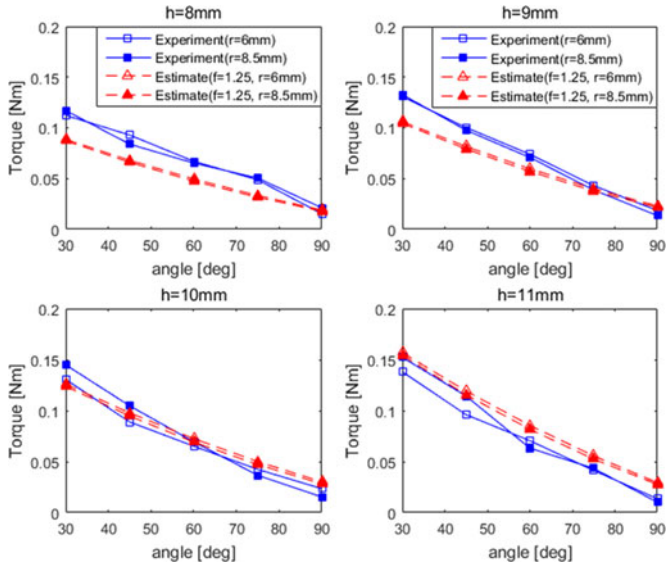

Fig. 14. Comparison of modeling and experimental results for actuator bending torque over finger angle, at 300 kPa.

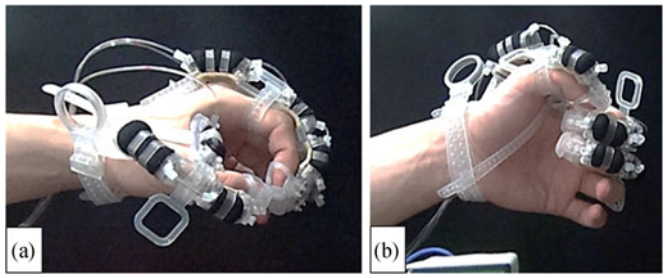

Fig. 15. Grasping posture. (a) General grasp, (b) Lateral pinch grasp.

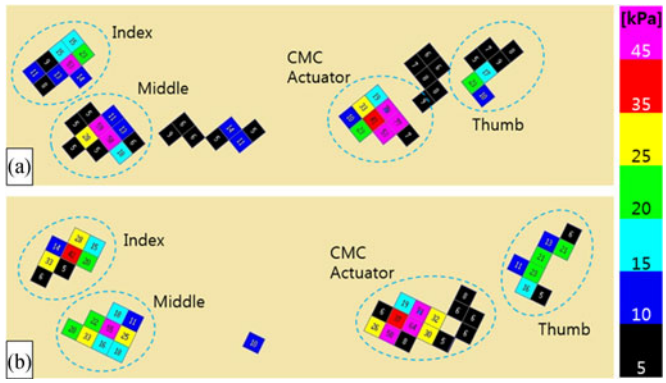

Fig. 16. Power grasp pressure measurement for cylindrical objects. (a) Diameter = 50 mm. (b) Diameter = 75 mm.

$$L_m \cong 2.5 + l + \alpha - r\sin\frac{\theta}{2} \tag{20}$$

By combining (3), (9), and (12)-(20), the bending torque can be obtained.

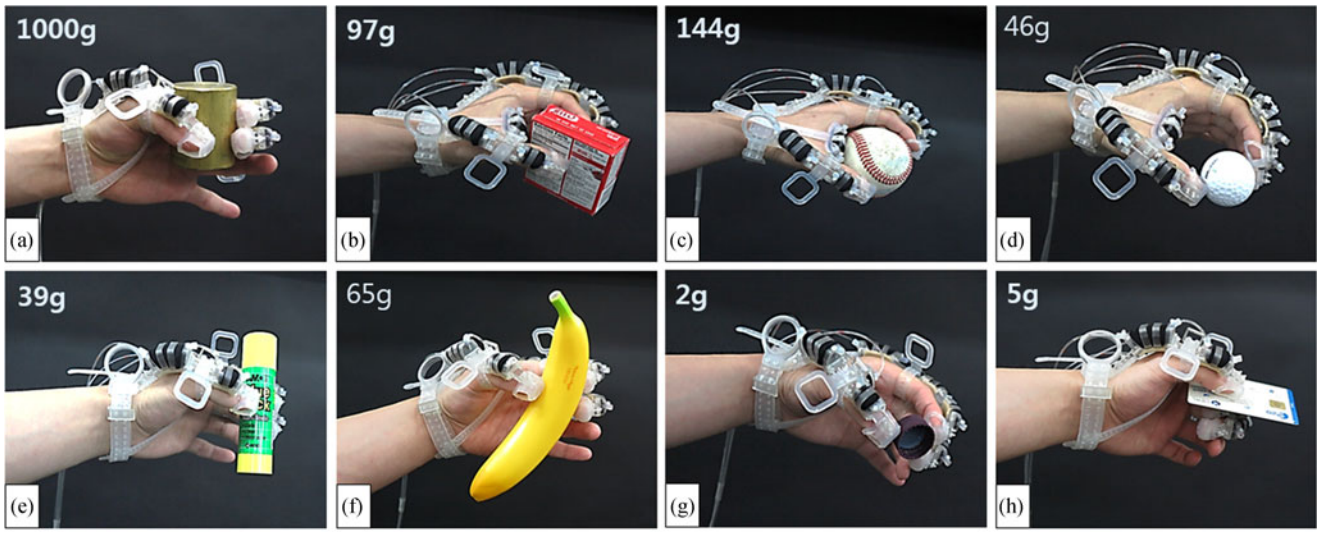

Fig. 17. Grasping tests with various objects. (a) 1kg weight, (b) small box, (c) baseball, (d) golf ball, (e) glue stick, (f) banana, (g) bottle cap, (h) credit card.

C. Comparison With Experiment Result

To evaluate the model's validity, we designed an experimental setup that mimics the condition of the DIP joint. The setup could change the joint angle by 0°-90° in 15° intervals. We made two versions of the setup to determine the effect of user hand size on module performance. Each setup has a 6 mm and an 8.5 mm joint radius (see Fig. 12).

Fig. 13 shows the modeling and experimental results for module bending torque over pressure at a 0° joint angle. Fig. 14 shows the modeling and experimental results for module bending torque over a joint angle and radius of 300 kPa (3bar). For both comparisons, the shapes are similar, but the modeling contains some errors, and the experimental results are not as linear as the estimated ones. Several factors may have led to these errors. First, the fabric was unable to perfectly restrict radial expansion of the tube. Second, when we attached the tunnel part to the rubber sheet, a small amount of adhesive permeated into gaps in the module, which changed the properties of the rubber sheet. Finally, we guess that the 100% modulus of VytaFlex 30 in datasheet did not perfectly match with Young's modulus of our range.

Although our modeling is not precise, it suggests a good direction for estimating actuator performance. According to the grasp force measure test described in Section V-B, we could see that an assistive glove using the smallest module ($h = 8$ mm) can hold a 1.1 kg cylindrical object, which is a level of performance sufficient to make the glove suitable for use in daily life [16]. Therefore, we used the smallest module ($h = 8$ mm) at the DIP and PIP joints in the experiments described in Section V.

V. Exo-Glove PM Performance

We conducted three experiments to evaluate glove performance, using healthy subjects with different hand sizes.

A. Hand Motion

We activated the modularized assistive glove under 0-300kPa (3bar) in the general grasp mode and the lateral pinch mode. Each motion was videorecorded.

In the general grasp mode [see Fig. 15(a)], every actuator is activated simultaneously, including the CMC joint actuator. The CMC joint is opened while all fingers are bent. This mode induces thumb abduction so that the user can hold a large object. The grasp posture is passively determined by the shape of the object (power grasp $\leftrightarrow$ pinch grasp).

In the lateral pinch mode [see Fig. 15(b)], every actuator is activated except the CMC joint actuator. The index and middle fingers are bent faster than the thumb because an air speed reducer is attached at the thumb actuator hose. In this mode the user can hold an object with the thumb (e.g., a card or a key).

At present, users with different hand stiffnesses show different hand motions for identical controls. This problem must be solved by further work on the glove.

B. Grasping Force Measurement

We measured pressure with a mat-type pressure sensor (160×160 mm^2 sensor; Pliance Hand Mat Sensor, Novel Inc., Germany) while a subject wearing the assistive glove grasped a cylindrical object at 300 kPa actuating pressure (see Fig. 16). The purpose of this measurement was to estimate the maximum manageable weight. The measurement was conducted using cylindrical objects with diameters of 50 mm and 75 mm. The measured normal forces were 22.35 N and 22.575 N for the 50 mm and 75 mm objects, respectively. Assuming that the friction coefficient is 0.5, the assistive glove can hold a cylindrical object weighing about 1.1 kg with a power grasp motion.

According to the pressure measurement plots in Fig. 16, we can see that grasp force occurred not only at the fingertips but also at the CMC actuator. Because the CMC actuator is also covered with silicone, it contributes to the maximum affordable weight of the glove.

Also, through the measurement process, we confirmed that a wearer can hold cylinders with a diameter of 50 mm weighing 500 g and 1 kg for 3 seconds and 12 seconds, respectively, and cylinders of the same weights but with a diameter of 75 mm for 1 second and 8 seconds, respectively, when assuming a 0.5 friction coefficient.

C. Grasping Various Objects in Daily Life

We conducted a third experiment to evaluate the performance of the assistive glove in grasping various objects. Three subjects, all wearing an assistive glove that they had personally customized according to formulas (1) and (2), placed eight objects into a box. The subjects had different hand lengths (167 mm, 190 mm, and 205 mm). Each motion is recorded at attached video.

Various hand postures were employed during the experiment, according to object shape and size (see Fig. 17). Large cylinders were held by a power grasp and small cylinders by a pinch grasp. Most of the objects were held in the general grasping mode (a-g), but the credit card (h) was held in the lateral pinch mode. Every object in the test was stably held, and none slipped down when the subjects moved their hand.

VI. Discussion

In this letter, we suggest a new concept for a customizable assistive glove, Exo-Glove PM, which is composed of small pneumatic actuator modules. Using small modules allowed us to achieve our two prime goals: low-cost customization and easy repair.

We developed a design and fabrication process for the actuator modules and introduced a method for estimating bending torque in different-size modules. Furthermore, we developed a customization method that does not require additional work during the manufacturing process.

To ensure good force transmission performance, we used both soft and rigid materials in the glove. Doing this allowed connector size to be minimized, which is important for allowing the glove to be fit to a wide range of hand sizes.

Certain problems remain to be solved for this assistive glove. First, in the pinch grasp posture, the fingertips tend to roll inside, which causes the finger to roll cylindrical objects at high pressure. This problem will be solved by decoupling the DIP/PIP actuators and the MCP actuator. In particular, in future we plan to control each joint module separately in order to attain various hand postures. To enable control, small bending sensors will be embedded in the modules.

Second, glove performance differs depending on the stiffness of the user's hand (which varies with such factors as muscle mass). Therefore, we need to include hand stiffness as a customization variable.

The formulas that we used to find spacer length—(1) and (2)—are not optimal. We will develop an improved spacer length equation and employ an advanced measuring tool in future work.

Finally, the actuators are not perfectly attached to the fingers (especially at their backs) and separate from the fingers when the user grasps a large object. To prevent this, we need to increase the contact area of the straps and add an additional strap at the back of the hand, but these changes could reduce wearability and customizability. To solve this problem, we need to attain a deeper understanding of hand structure.

Reference

[1] SEM^{TM} Glove, "Bioservo technologies AB," 2017. [Online]. Available: http://bioservo.com/healthcare/product-portfolio/sem-glove/.

[2] PAH-110, 株式会社　エルエーピー, 2016. [Online]. Available: http://www.lap-shop.jp/

[3] B. L. Shields, J. A. Main, S. W. Peterson, and A. M. Strauss, "An anthropomorphic hand exoskeleton to prevent astronaut hand fatigue during extravehicular activities," *IEEE Trans. Syst., Man Cybern.-Part A, Syst. Humans*, vol. 27, no. 5, pp. 668–673, Sep. 1997.

[4] A. Wege and G. Hommel, "Development and control of a hand exoskeleton for rehabilitation of hand injuries," in *Proc. IEEE/RSJ Int. Conf. Intell. Robots Syst.*, 2005, pp. 3046–3051.

[5] I. Sarakoglou, A. Brygo, D. Mazzanti, N. G. Hernandez, D. G. Caldwell, and N. G. Tsagarakis, "HEXOTRAC: A highly under-actuated hand exoskeleton for finger tracking and force feedback," in *Proc. IEEE/RSJ Int. Conf. Intell. Robots Syst.*, 2016, pp. 1033–1040.

[6] Y. Yun, P. Agarwal, J. Fox, K. E. Madden, and A. D. Deshpande, "Accurate torque control of finger joints with UT hand exoskeleton through Bowden cable SEA," in *Proc. IEEE/RSJ Int. Conf. Intell. Robots Syst.*, 2016, pp. 390–397.

[7] B. B. Kang, H. Lee, H. In, U. Jeong, J. Chung, and K.-J. Cho, "Development of a polymer-based tendon-driven wearable robotic hand," in *Proc. IEEE Int. Conf. Robot. Autom.*, 2016, pp. 3750–3755.

[8] P. Polygerinos, Z. Wang, K. C. Galloway, R. J. Wood, and C. J. Walsh, "Soft robotic glove for combined assistance and at-home rehabilitation," *Robot. Auton. Syst.*, vol. 73, pp. 135–143, 2015.

[9] H. K. Yap, B. W. Ang, J. H. Lim, J. C. Goh, and C.-H. Yeow, "A fabric-regulated soft robotic glove with user intent detection using EMG and RFID for hand assistive application," in *Proc. IEEE Int. Conf. Robot. Autom.*, 2016, pp. 3537–3542.

[10] J.-H. Low, M. H. Ang, and C.-H. Yeow, "Customizable soft pneumatic finger actuators for hand orthotic and prosthetic applications," in *Proc. IEEE Int. Conf. Rehabil. Robot.*, 2015, pp. 380–385.

[11] M. Haghshenas-Jaryani, W. Carrigan, C. Nothnagle, and M. B. Wijesundara, "Sensorized soft robotic glove for continuous passive motion therapy," in *Proc. 6th IEEE Int. Conf. Biomed. Robot. Biomechatron.*, 2016, pp. 815–820.

[12] H. K. Yap, J. H. Lim, F. Nasrallah, J. C. Goh, and R. C. Yeow, "A soft exoskeleton for hand assistive and rehabilitation application using pneumatic actuators with variable stiffness," in *Proc. IEEE Int. Conf. Robot. Autom.*, 2015, pp. 4967–4972.

[13] S. W. Kwok *et al.*, "Magnetic assembly of soft robots with hard components," *Adv. Funct. Mater.*, vol. 24, pp. 2180–2187, 2014.

[14] J. Germann, M. Dommer, R. Pericet-Camara, and D. Floreano, "Active connection mechanism for soft modular robots," *Adv. Robot.*, vol. 26, pp. 785–798, 2012.

[15] J.-Y. Lee, W.-B. Kim, W.-Y. Choi, and K.-J. Cho, "Soft robotic blocks: Introducing SoBL, a fast-build modularized design block," *IEEE Robot. Autom. Mag.*, vol. 23, no. 3, pp. 30–41, Sep. 2016.

[16] K. Matheus and A. M. Dollar, "Benchmarking grasping and manipulation: Properties of the objects of daily living," in *Proc. IEEE/RSJ Int. Conf. Intell. Robots Syst.*, 2010, pp. 5020–5027.